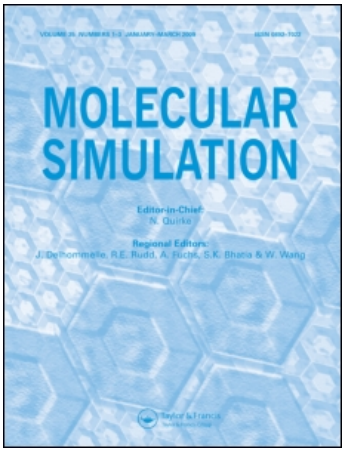

Molecular Simulation
Publication details, including instructions for authors and subscription information:
http://www.informaworld.com/smpp/title~content=t713644482

The solution structures of the HIV protease inhibitor DG35-VIII

Jason Dang[a]; Susan Blandford[a]; Maruse Sadek[a]; D. Grobelny[b]; Robert T. C. Brownlee[a]
[a] Department of Chemistry, La Trobe University, Vic., Australia [b] Narhex Operations Pty Ltd, c/o Department of Chemistry, La Trobe University, Vic., Australia

Online publication date: 26 October 2010

To cite this Article Dang, Jason , Blandford, Susan , Sadek, Maruse , Grobelny, D. and Brownlee, Robert T. C.(2002) 'The solution structures of the HIV protease inhibitor DG35-VIII', Molecular Simulation, 28: 8, 827 — 843
To link to this Article: DOI: 10.1080/0892702021000002511
URL: http://dx.doi.org/10.1080/0892702021000002511

Molecular Simulation, 2002 VOL. 28 (8–9), pp. 827–843

THE SOLUTION STRUCTURES OF THE HIV PROTEASE INHIBITOR DG35-VIII

JASON DANG[a,*], SUSAN BLANDFORD[a], MARUSE SADEK[a], D. GROBELNY[b] and ROBERT T.C. BROWNLEE[a]

[a]*Department of Chemistry, La Trobe University, Vic. 3086, Australia;* [b]*Narhex Operations Pty Ltd, c/o Department of Chemistry, La Trobe University, Vic. 3086, Australia*

(Received May 2001; In final form November 2001)

NMR spectroscopy techniques have been used to determine the conformation of DG35-VIII in DMSO, acetone, and methanol. COSY and Heteronuclear Correlation experiments were used to confirm the proton spectral assignments. NOESY experiments were used to identify proton internuclear distances which were used to determine the 3D structure. The NOESY data identified a single "U-shaped" conformer of DG35-VIII in acetone, and an alternate "extended" conformer in methanol and two possible conformations in DMSO. Restrained molecular minimization methods using the Molecular Mechanics Program "DISCOVER" and "DYANA" were used to determine a low energy structure consistent with the NMR data.

The extended structure of DG35-VIII was compared with closely related HIV protease inhibitors (VX-478 and ABT-538) and showed similar backbone structures, with the functional isostere groups superimposed on each other. The binding energy of DG35-VIII with HIV protease was examined and found to be comparable with VX-478 and ABT-538.

Keywords: HIV protease inhibitor; Nuclear Overhauser effect; Molecular modeling; Nuclear magnetic resonance

INTRODUCTION

Much effort has been directed to the development of peptidic based inhibitors of the aspartyl protease, HIV protease, to control AIDS [1–4]. There are large number of such compounds that bind to HIV protease in the nano to micro molar

*Corresponding author.

ISSN 0892-7022 © 2002 Taylor & Francis Ltd
DOI: 10.1080/0892702021000002511

range yet show structural variation and conformational mobility [5]. On the other hand X-ray structures of many of these compounds bound to HIV protease show a remarkably similar binding motif, thus requiring a pre-organization of the drug from its lowest energy conformation to the binding conformation. One way of minimizing this energy loss is to pre-organize the drug into the appropriate binding structure [5]. Another is to design compounds that have their lowest energy structure similar to the bound structure. In either case an experimental determination of the solution structure of such drugs in solution is of value.

This paper reports the solution structure and a binding study of DG35-VIII, an HIV protease inhibitor, in a range of solvents using NMR spectroscopic methods and molecular modeling. This drug, like several others, is based on mimics of the natural peptide substrate but having a peptide mimetic isostere which binds strongly to the receptor site and blocks access of the natural peptide from this receptor. Figure 1 illustrates the hydroxyethylhydrazide isostere which binds to the active site of the enzyme, but resists bond cleavage by the protease enzymes. DG35-VIII has been found to inhibit HIV-l protease [6], with 50% inhibitor concentration (IC_{50}) in the nanomolar range.

EXPERIMENTAL METHODS

The sample DG35-VIII [6] was made up of 5 mg of sample in 0.6 ml of each solvent, giving concentrations of 0.0137 M. Since this drug is insoluble in water structures were determined in methanol, acetone, and dimethyl sulfoxide. The data was collected using a Bruker Avance 400 MHz NMR Spectrometer. Experimental procedures are shown in the Appendix A. The samples were degassed using several freeze/thaw cycles and sealed under vacuum to remove any paramagnetic oxygen. The NOESY spectra were recorded at different mixing times to determine that the intensities were not influenced by spin diffusion.

The application of restrained energy minimization using the NOE distance constraints from NMR experiments resulted in the 3D structure. The intensities of the NOE interactions are integrated and converted into distances classified as strong (1.8–3 Å), medium (3–4 Å) and weak (4–6 Å) [7]. The ROESY spectrum was obtained but showed no additional data to that obtained by the NOESY experiment. The NOE cross peaks on both side of the diagonal line were averaged and calibrated against known cross peaks. Two protons attached to the quinoline ring, H4″ and H5″ were chosen for this calibration as they have a fixed separation of 2.54 Å obtained from model building and X-ray data. All other NOE data were standardized against this value using the method suggested by Derome [8].

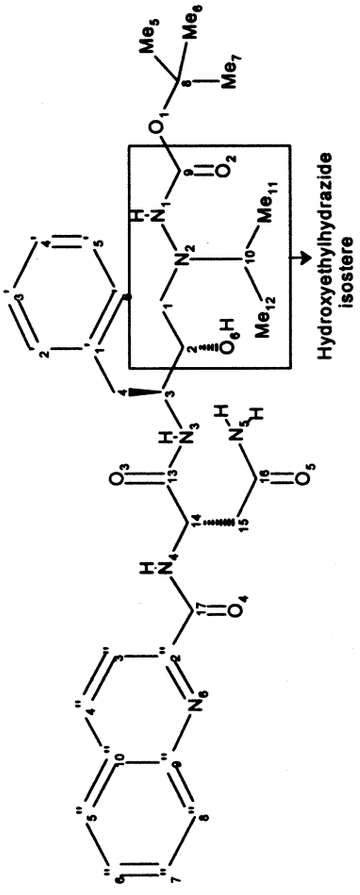

FIGURE 1 Chemical structure of DG35-VIII showing the accepted numbering systems.

Initial structure of DG35-VII was created using DYANA [9] package. This program calculates the 3D protein and nucleic acid structures on the basis of conformational restraints derived from the NMR experiments, which uses simulated annealing combined with molecular dynamics in torsion angle space. The Dyana software builds structures from a library of known amino acids, thus for this molecule two peptidic type components were constructed and inserted into the Dyana library.

RESULTS AND DISCUSSION

NMR data and structural calculations were performed on DG35-VIII in acetone, methanol and DMSO solutions. In acetone a single structure was seen, whereas in methanol and DMSO multiple conformations were evident. Initially the structure in acetone solvent is discussed.

The proton spectrum of DG35-VIII in acetone is shown in with the aromatic and the amide protons appearing between 6 and 7.5 ppm while the quinoline ring appeared slightly downfield between 7.5 and 8.6 ppm. The aliphatic group of the tertiary butyl group appeared at 1.36 ppm. The two doublets at 0.9–1.0 ppm are overlapped and appear as a triplet, indicating the protons on the isopropyl methyl carbons are non-equivalent. A comparison of chemical shifts in DMSO and methanol shows similarities between the peaks with only slight shifts of the NH protons. In D4-methanol the amide protons disappear as they exchanged with the -OD in the methanol solvent. The NH protons are extremely useful for assignment purposes and in NOE data, thus spectra were measured in D3-methanol using a pre-saturation pulse sequence experiment, where a weak transmitter pulse p1 of 2 s is used for irradiation and consequently suppress the huge solvent signal. A difficult region to unravel, see Fig. 2, is 2.7–3.2 ppm where there are geminal protons (H4, H15, H1) overlapping each other. Careful use of the COSY data allows the chemical shifts to be assigned but useful coupling information had to be retrieved from additional J-Resolved [10] experiments.

Assignment of the aromatic protons was accomplished using a combination of known and predicted ^{13}C shifts [11]; DEPT experiment and the standard carbon–proton correlation HSQC experiment. The ^{13}C assignment of C4″ in acetone to 137.26 ppm, this allowed the proton assignment of H4″ at 8.55 ppm.

The complete assignment in methanol and DMSO followed closely the method describes above and the assignments of the proton and carbon spectra are shown in Table I.

TABLE 1 Proton and Carbon Chemical shifts

	Acetone δ ppm	*Methanol* δ ppm	*DMSO* δ ppm
Proton			
H11(1), H11(2), H11(3)	1.02	0.91	0.86
H12(1), H12(2), H12 (3)	1.03	0.95	0.88
H5(1–3), H6(1–3), H7(1–3)	1.39	1.36	1.32
H1(1)	2.52	2.46	2.49
H1(2)	2.52	2.58	2.49
H15(1)	2.83	2.82	2.63
H4(1)	2.85	2.84	2.74
H15(2)	2.90	2.83	2.76
H4(2)	2.95	2.85	2.83
H10	3.02	2.90	2.83
H2	3.59	3.53	3.42
H3	4.05	4.02	3.98
H6	4.38	Exchanged	4.43
H14	4.95	4.90	4.82
HN5(1)	6.34	6.87	6.96
HN1	6.74	7.46	7.69
HN5(2)	7.00	6.99	7.46
H3′, H5′	7.11	7.08	7.18
H4′	7.20	6.98	7.08
H2′, H6′	7.26	7.18	7.16
HN3	7.38	7.78	7.75
H6″	7.74	7.67	7.71
H7″	7.89	7.82	7.87
H5″	8.08	7.98	8.07
H8″	8.19	8.15	8.14
H3″	8.28	8.18	8.17
H4″	8.55	8.46	8.57
HN4	9.29	9.36	9.13
Carbon			
C11	X	15.48	17.59
C12	X	X	19.14
C5, C6, C7	X	26.85	28.1
C1	51.95	57.78	56.5
C15	X	36.07	37.35
C4	X	37.19	37.79
C10	50.15	55.71	55.42
C2	X	X	66.51
C3	37.95	52.56	51.8
C8	X	78.89	78.31
C14	36.76	50.45	50.44
C4′	125.54	125.35	125.84
C2′, C6′	129.00	128.97	129.13
C3′, C5′	127.59	127.19	128.03
C6″	127.76	127.64	128.16
C7″	129.90	129.73	130.58
C5″	127.71	127.47	128.09
C8″	129.30	129.08	129.17
C3″	118.22	117.76	118.52
C4″	137.26	137.16	137.92
C1′	138.67	137.86	138.76
C2″	149.54	148.49	149.48
C9″	146.24	146.14	145.91
C10″	129.06	128.63	128.9
C9	X	X	156.75
C13	169.74	170.93	170.13
C16	171.89	173.23	171.62
C17	163.57	164.69	163.48

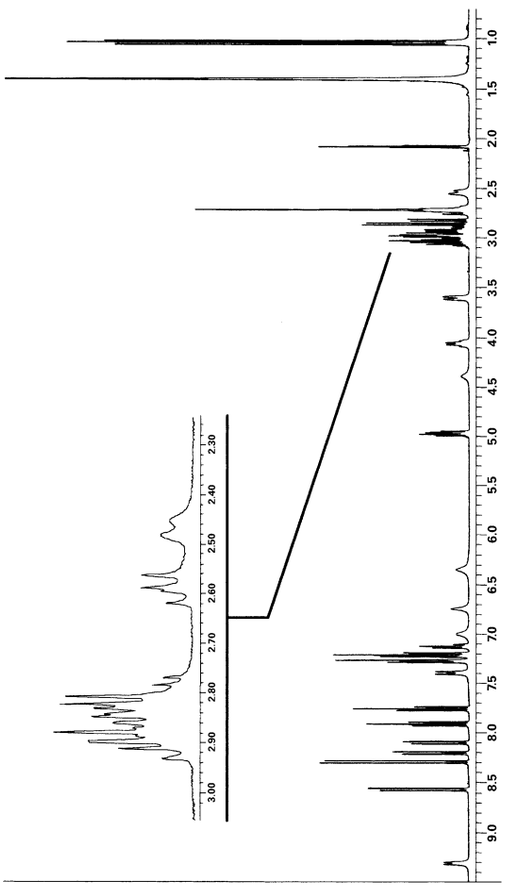

FIGURE 2 Proton spectrum of DG35-VIII in acetone at 313 K.

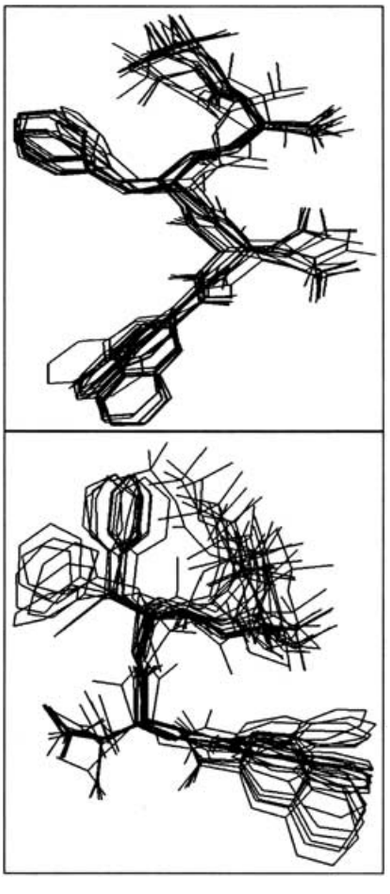

FIGURE 3 Twenty "U" shaped structures from acetone (left) and "extended" structures in methanol (right) solvents.

In each solvent NOESY spectra were used to identify a series of distance constraints. Additional coupling constants restraints derived from NH to C-α angle constraints measured from the 1-D spectra [12] were obtained. The distance constraints were categorized into strong, medium or weak according to the volume integrated intensity [7]. The constraints are shown in Appendix B.

In all the solvent systems the intensities of the NOE peaks were opposite that of the diagonal peaks indicating that DG35 has a short correlation time. In order to check that NOE data was not lost as result cross over point between correlation time and NOE intensity ROESY spectroscopy experiments were also performed. No additional peaks were observed.

MOLECULAR MODELING

Energetic calculations were performed on a Silicon Graphics Irix Indigo workstation using MSI software [13] (INSIGHT II, DISCOVER, DOCKING) with the Molecular Simulations consistent valence forcefield (CVFF) and submitted to a structural optimization using 2000 steps of energy minimization with the steepest descent and conjugate gradients algorithms. The first step utilized the steepest descent method; subsequent steps used conjugate gradients with derivative of 0.001. Each step was run until the convergence with the designated derivative was achieved.

Visual inspection of the NOE data, refer to Appendix B, in the three solvents shows that the structure of DG-35 is different in each solvent system. In acetone there are a large number of NOE constraints consistent with a highly organized structure in which the backbone of the structure is "U" shaped. For example there are NOEs from the naphthalene ring to the isopropyl group. On the other hand, in methanol the constraints are predominantly between the phenyl and tertiary-butyl groups with no NOE cross peaks between the quinoline group and the rest of the molecule indicating of an "extended" structure. Finally in DMSO it is clear that both the "extended" and "U" structures are present which are not consistent with a single structure and thus the use of these NOE constraints to build structures would require an assignment of the NOE constraint data into at least two groups.

This intuitive analysis is confirmed from the analysis using the DYANA package to generate structures. In acetone 20 "U" shaped structures are generated which after energy minimization resulted in a total molecular energy of 47.14 Kcal/mole and as expected the quinoline ring is reasonably close to the isopropyl group. On the other hand in methanol the use of the NOE constraints in DYANA generated "extended structures", refer to Fig. 3, somewhat similar to the 2D chemical representation in Fig. 1. Unexpectedly, energy minimization of

these structures resulted in some minimizing to the "U" shaped structure described above and others minimizing to the "extended" structure with an energy of 44.20 Kcal/mole. This result is indicative of a complex energy barrier between the "U" shaped and "extended" structures resulting in the structure obtained being dependent on which side of the barrier the initial structures started. This extended structure of DG35-VIII is similar to the crystal structure of a range of related inhibitors [14].

In DMSO solvent, there were NOE interactions between both the isopropyl and phenyl groups and the quinoline end of the molecule. This results in impossible structural determination and unrealistic energetic calculations due to violations and straining of the molecule. Therefore physical classification of the NOEs into two groups was performed which resulted in two conformations for DG35-VIII in DMSO: these are very similar to the "U" shape and "extended" structures discussed above.

SUPERIMPOSING DG35-VIII WITH KNOWN DRUGS

Recent studies of X-ray crystal structures of 12 substrate-based peptidic inhibitors [5] showed similarities in their binding mode despite their structural diversity and conformational flexibility. The aim of this part of the study was to examine the structures of DG35-VIII obtained in methanol and acetone solution and compare these with literature structures. Two known inhibitors obtained from Protein Data Bank,[†] VX-478[‡] and ABT-538,[¶] which have the similar isosteric groups to DG35-VIII were selected for this study. These two inhibitors were extracted from the complete crystal file of inhibitor/protease structure. The superimposition of the backbone of the DG35-VIII "extended" structure in methanol solution with both VX-478 and ABT-538 was performed by overlapping the heavy atoms. The result shows clearly the similarities in these structures, see Fig. 4.

On the other hand, it is obvious that the "U" shaped structure of DG35-VIII derived from the NMR data in acetone does not overlap with the VX-478 nor ABT-538.

[†]http://pdb.wehi.edu.au:8181/pdb/
[‡]pdb accession code: 1 hpv.
[¶]pdb accession code: 1 hxw.

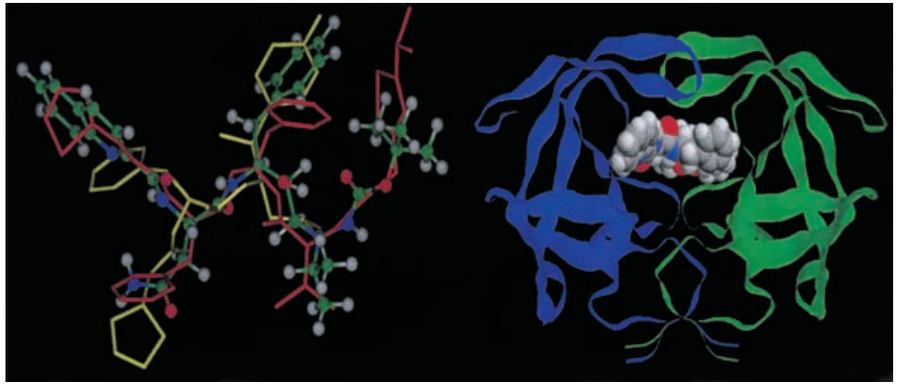

FIGURE 4 DG35 (Ball and Stick) superimposing with two known HIV drugs VX-478 and ABT-538; and as a Space fill display in the active site of HIV protease (right).

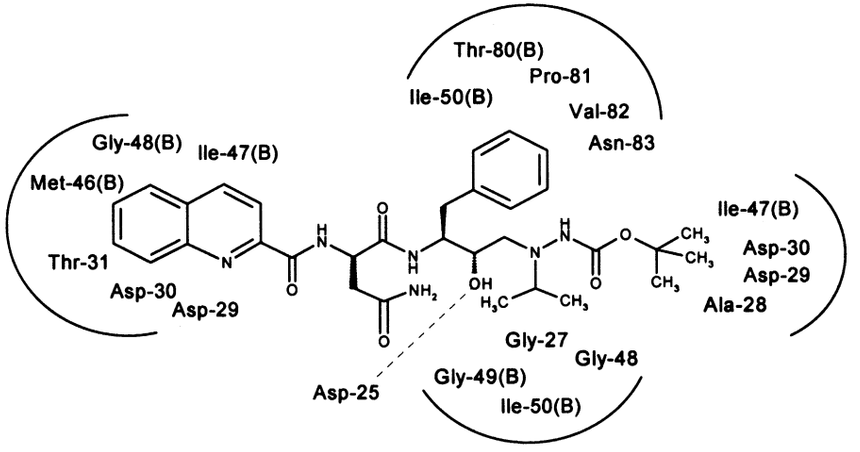

FIGURE 5 Diagrammatic presentation of DG35-VIII in the active site of HIV protease. (B) indicates that the residues are in the back of DG35-VIII.

BINDING STUDY

Since no X-ray structures of this drug with HIV protease are available a model was constructed in order to examine the binding of DG35-VIII to the active site of the HIV protease. A similar study [15] of the interactions obtained from the X-ray structure of VX-478 complexed with HIV-1 protease identified four binding pockets and identified hydrogen bonds between the drug and Asp-25 and solvation within the pockets.

Figure 3 illustrates DG35-VIII occupying the active site of HIV protease. This model was constructed by overlapping DG35 with VX-478 in order to obtain the initial coordinates for DG35-VIII in the active site. VX-478 was then removed and the DG35-VIII/HIV protease complex was minimized. A careful examination of the active site would give a better understanding of how DG35-VIII binds to HIV protease, and identifies hydrogen bonding with available water molecules and the hydrophobic pockets. Since the DG35-VIII structure in methanol was superimposable with VX-478, the expected binding pockets for DG35-VIII should be the generally similar to VX-478, based on the similarities in the results of the calculated binding energies and backbone structures. As expected, it was found that DG35-VIII positioned itself slightly differently to

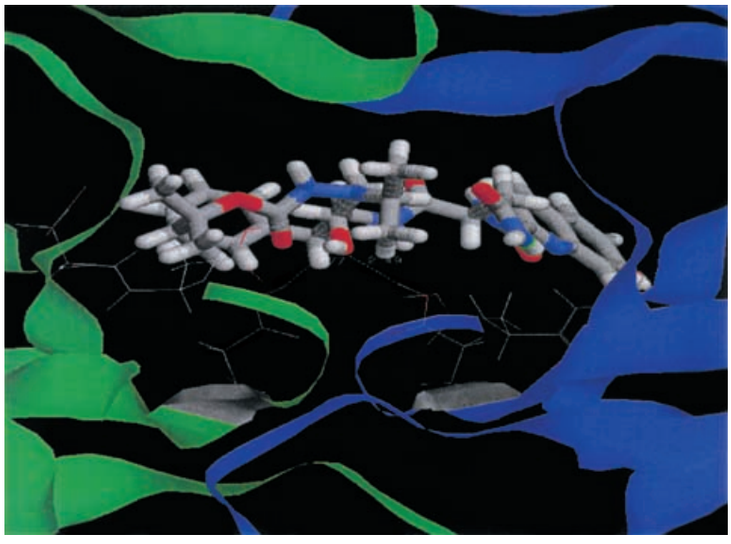

FIGURE 6 A visual study of DG35-VIII showing H-bonding with Asp25 of HIV protease.

VX-478 in the active site as a result of the different steric/electronic properties, however the overall features are very similar.

The hydrophobic phenyl group in DG35-VIII is largely in contact with the hydrophobic amino acids including Isoleucine 50, Proline 81 and Valine 82. In the naphthalene pocket it was found that Isoleucine 47 situated on the top surface close to 4″ and 5″ carbons of DG35-VIII, whereas Aspartic acid 30 and 29 stabilized the polar Nitrogen 6. The tertiary butyl group on DG35-VIII was surrounded by Ala-28 and Ile-47 with Aspartic acid 29 and 30 situated close by. Glycine 49 surrounded the isostere of DG35-VIII in the rear and with Alanine 28, Glycine 27 and 48 in front, see Fig. 5.

The Aspartyl residue (Asp-25) showed a hydrogen bond to the hydroxyl in DG35-VIII in the same way as seen in VX-478, highlighted in Fig. 6. There are three water molecules hydrogen bonded to $O_{(3)}$, $O_{(5)}$ and $N_{(1)}$ in this vicinity.

CONCLUSIONS

Whereas X-ray diffraction studies provide a unique picture of the drug in the active site, this paper has used a combination of NMR spectroscopy and data from X-ray studies to show how a drug conformation changes in binding to the active site. The NMR data on DG35-VIII in solution identified two structures with similar energies of which only the "extended" structure bound to the active site of HIV protease since that structure was similar with the X-ray crystals structures of HIV protease inhibitors (VX-478 and ABT-538), with similar backbone structures and with the isosteric groups in each inhibitor superimposed.

References

[1] Slee, H.D., Laslo, L.K., Elder, H.J., Ollman, R.I., Gustchina, A., Kervinen, J., Zdanov, A., Wlodawer, A. and Wong, C. (1995) "Selectivity in the inhibition of HIV and FIV protease: inhibitory and mechanistic studies of pyrrolidine-containing α-keto amide and hydroxyethylamine core structure", *J. Am. Chem. Soc.* **117**, 11867–11878.

[2] Gante, J. (1994) "Peptide mimetics—tailor-made enzyme inhibitors", *Angew. Chem. Int. Ed. Engl.* **33**, 1699–1720.

[3] Tomasselli, A.G., Howe, W.J., Sawyer, T.K., Wlodawer, A. and Heinrikson, R.L. (1991) "The complexities of AIDS: an assessment of the HIV protease as the therapeutic target", *Chim. Oggi*, 6–27.

[4] Gait, M.J. and Karn, J. (1995) "Progress in anti-HIV structure-based drug design", *Trends Biotechnol.* **13**, 430–438.

[5] Reid, R.C., March, D.R., Dooley, M.J., Bergman, D.A., Abbenante, G. and Fairlie, D.P. (1996) "A novel bicyclic enzyme inhibitor as a consensus peptido-mimetic for the receptor-bound conformations of twelve peptidic inhibitors of HIV-1 Protease", *J. Am. Chem. Soc.* **118**, 8511–8517.

[6] Grobelny, D., Chen, Q., Tyssen, D., Tachedjian, G., Sebire, K., Buchanan, L. and Birch, C. (1997) "Antiviral activity of DG-35-VIII, a potent inhibitor of the protease of human immunodeficiency virus", *Antivir. Chem. Chemother.* **8**, 99–106.
[7] Clore, G.M., Brunger, A.T., Karplus, M., Gronenborn, A.M. (1986) "Application of molecular dynamics with interproton distance restraints to three-dimensional protein structure determination. A model study of crambin", *J. Mol. Biol.* **191**, 523–551.
[8] Derome, A.E. (1987) *Modern NMR Techniques for Chemistry Research* (Pergamon Press, Singapore).
[9] Gunter, P., Mumenthaler, C. and Wuthrich, K. (1997) "Torsion angle dynamics for NMR structure calculation with the new program DYANA", *J. Mol. Biol.* **273**, 283–298.
[10] Eberstadt, M., Gemmecker, G., Mierke, D.F. and Kessler, H. (1995) "Scalar coupling constants-their analysis and their application for the elucidation of structures", *Angew. Chem. Int. Ed. Engl.* **34**, 1671–1695.
[11] HIPPO CNMRS ^{13}C software, Prof. Helmut Honig, Institute of Organic Chemistry Technical, University of Graz.
[12] McManus, A.M., Nielson, K.J., Marcus, J.P., Harrison, S.J., Green, J.L., Manners, J.M. and Craik, D.J. (1999) "MiAMP1, a novel protein from macadamia integrifolia adopts a Greek key β-barrel fold unique amongst plant antimicrobial proteins", *J. Mol. Biol.* **293**, 629–638.
[13] Biosym/MSI San Diego California 1997.
[14] Nair, C.A., Miertus, S., Tossi, A. and Romeo, D. (1998) "A computational study of the resistance of HIV-1 aspartic protease to the inhibitors ABT-538 and VX-478 and design of new analogs", *Biochem. Biophys. Res. Commun.* **242**, 545–551.
[15] Kim, E.E., Baker, C.T., Dwyer, M.D., Murcko, M.A., Rao, B.G., Tung, R.D. and Navia, M.A. (1995) "Crystal structure of HIV-1 protease in complex with VX-478, a potent and orally bioavailable inhibitor of the enzyme", *J. Am. Chem. Soc.* **117**, 1181–1182.
[16] Werner, M.H., Bruker Avance User's Guide, 1994.

APPENDIX I: NMR EXPERIMENTAL PROCEDURES

The standard 1D proton experiments were run at 400 MHz with four dummy scans and eight scans. In general 32 K data points were acquired with the spectral width of 4400 Hz. The temperature for all of the runs was controlled at 298 K except for the acetone sample, which used 313 K because the sample was sparingly soluble. The number of scans used in the standard ^{13}C experiments was 10^4 and 16 K data points were collected. The 90° pulse used was 6.00 μs and the relaxation delay was 2.00 s. The gradient COSY was run with eight scans in each of the 256 experiments, using the pulse sequences "cosygs" and "cosyprtp" for presaturated experiment in D3-methanol. The 90° pulse was 10.20 μs and the recovery delay was 2.00 s. Only real data points were sampled and processed by real Fourier transform. The FID was processed with 1 K data points in the F2 projection and with 256 data points in the F1 projection.

The HSQC spectrum was obtained using 32 scans in each of the 256 experiments using the pulse sequence "invigstp" was used and the 90° pulse was 11.10 μs for ^{1}H and 11.00 μs for ^{13}C. The delay for gradient recovery was 100 μs

and the relaxation delay was 1.60 s. The FID was then processed with 2 K data points in F2 and 1 K data points in F1.

NOESY were applied with 256 experiments with 64 scans, using the Bruker pulse sequence [16] "noesytp" for acetone and "noesyprtp" for presaturated D3-methanol. Mixing times between 400 and 900 ms were used to collect data with 900 ms giving the most useful information. The relaxation delay was 2 s and 1 K and 512 data points were processed in F2 and F1 axes, respectively. The ROESY experiments were set up in the same way.

APPENDIX II: NOESY CROSS-PEAKS OBSERVED FOR DG35-VIII

TABLE AI NOESY cross-peaks observed for DG35-VIII in acetone, methanol and DMSO at 400 MHz

Label Hi	*Label Hj*	*Calculate distance A*	*Class of NOE*
NOESY cross peaks observed for DG35-VIII in acetone at 400 MHz			
Isopropyl	3″	5.08	Weak
Isopropyl	N1	3.52	Medium
Tbu	6′	3.96	Weak
Tbu	N1	4.89	Weak
Isopropyl	H10	2.91	Strong
Isopropyl	H1A	3.80	Medium
Isopropyl	H1B	3.99	Weak
H4	2′	2.22	Strong
HN3	H15A	2.60	Strong
H3	6′	2.55	Weak
H14	HN3	2.57	Medium
H14	HN4	2.92	Strong
N1	H1A	2.81	Weak
HN4	H15A	3.13	Medium
HN4	H15B	3.06	Medium
HN3	HN4	3.01	Strong
4″	**5″**	**2.54**	**Strong**
H2	H3	2.42	Strong
H3	H1A	2.53	Strong
H14	H15A	2.58	Medium
H14	H15B	2.65	Strong
H3	H1B	2.73	Strong
H2	H1B	2.72	Strong
H2	H4	2.72	Strong
H2	OH	2.75	Strong
NOESY cross peaks observed for DG35-VIII in methanol at 400 MHz			
Isopropyl	H1A	3.56	Medium
Isopropyl	H1B	4.30	Weak
H1	H2	3.84	Strong
H1	H3	3.65	Strong
H3	H2	2.39	Strong
Isopropyl	N1	2.66	Medium

TABLE AI – *continued*

Label Hi	*Label Hj*	*Calculate distance A*	*Class of NOE*
Tbu	6′	2.73	Weak
N1	H1A	2.80	Strong
N1	H1B	3.19	Medium
N1	H2	3.09	Medium
4″	**5″**	**2.54**	**Strong**
N3	H4	2.58	Strong
N3	H2	3.31	Medium
N3	H3	2.83	medium
H4	*O*-Phenyl	2.29	Strong
HN4	H15	3.12	Medium
HN4	H14	2.85	Strong
N3	H14	2.49	Medium
N3	N4	2.93	Weak
NOESY cross peaks observed for DG35-VIII in DMSO at 400 MHz			
Isopropyl	TBu	4.83	Weak
Isopropyl	Isopropyl	3.57	Medium
Isopropyl	H10	2.67	Strong
Isopropyl	H2	4.14	Weak
Isopropyl	H6	4.19	Weak
10	tBu	4.03	Weak
2	tBu	3.97	Medium
6	tBu	4.06	Weak
14	tBu	4.38	Weak
Isopropyl	H10	2.74	Strong
Isopropyl	H2	3.27	Medium
Isopropyl	H3	3.13	Medium
Isopropyl	H6	3.44	Medium
H15A	H3	2.15	Strong
H15A	H2	2.68	Strong
H4A	H3	2.80	Strong
H10	H6	2.67	Strong
H4B	H14	2.69	Strong
H4B	H6	3.02	Medium
H15B	H14	2.59	Strong
H2	H3	3.03	Medium
H2	H6	2.72	Strong
H8″	HN4	3.44	Medium
H3″	H4″	2.47	Strong
H5″	H4″	2.42	Strong
H2′/6′	H8″	3.25	Medium
H3′/5′	H5″	3.35	Medium
HN5A	H14	3.33	Medium
H3′/5′	H14	3.07	Medium
HN5B	H14	3.24	Medium
HN3	H14	3.15	Medium
H3″	H14	3.05	Medium
H4″	H14	3.17	Medium
HN4	H14	2.84	Strong
H3′/5′	H3	2.58	Strong
HN3	H3	3.09	Medium
H7″	H3	3.06	Medium
H3′/5′	H2	3.13	Medium
HN1	H2	2.47	Strong

TABLE AI – *continued*

Label Hi	*Label Hj*	*Calculate distance A*	*Class of NOE*
H3′/5′	H4A	2.51	Strong
HN1	H10	2.89	Strong
H3″	H4A	2.95	Strong
HN4	H15B	2.82	Strong
HN4	H15A	3.17	Medium
HN3	H15B	2.72	Strong
HN5B	H15B	2.86	Strong
H3′/5′	H4A	2.69	Strong
HN5A	H15B	2.95	Strong
HN5A	H15A	3.23	Medium
HN5B	H15A	3.20	Medium
HN3	Isopropyl	3.49	Medium
H2′/6′	TBu	4.13	Weak
H3′/5′	TBu	3.98	Medium
HN1	TBu	3.90	Medium
H3″	TBu	4.10	Weak
H4″	TBu	4.09	Weak
H3′/5′	Isopropyl	3.96	Medium
HN1	Isopropyl	3.29	Medium
H3″	Isopropyl	3.80	Medium
H4″	Isopropyl	3.99	Medium